ARTICLE

Raman and Fluorescence Spectroscopic Studies of a DNA-Dispersed Double-Walled Carbon Nanotube Solution

Jin Hee Kim,[†] Masakazu Kataoka,[†] Daisuke Shimamoto,[†] Hiroyuki Muramatsu,[‡] Yong Chae Jung,[†] Takuya Hayashi,[†] Yoong Ahm Kim,[†,*] Morinobu Endo,[†,‡] Jin Sung Park,[§] Riichiro Saito,[§] Mauricio Terrones,[⊥,∥,▽] and Mildred S. Dresselhaus[#]

[†]Faculty of Engineering, Shinshu University 4-17-1 Wakasato, Nagano, 380-8553, Japan, [‡]Institute of Carbon Science and Technology, Shinshu University, 4-17-1 Wakasato, Nagano, Japan, [§]Department of Physics, Tohoku University, Sendai, 980-8578, Japan, [⊥]The Department of Physics and Mathematics, Division of Science, Arts and Technology, Universidad Iberoamericana, Avenida Prolongación Paseo de la Reforma 880, Santa Fé 012100, DF, México, [∥]Departamento de Ciencia e Ingeniería de Materiales e Ingeniería Química, Escuela Politécnica Superior, Universidad Carlos III de Madrid, Avenida Universidad 30, 28911 Leganés, Madrid, Spain, and [#]Massachusetts Institute of Technology, Cambridge, Massachusetts 02139-4307. [▽]Current affiliations..

ABSTRACT We performed resonant Raman/fluorescence spectroscopic studies on double-walled carbon nanotubes (DWNTs) that were dispersed in an aqueous single stranded DNA solution. The luminescence signals from the inner tubes of DWNTs are intensified in the isolated state of each individual DWNT. The completely depressed radial breathing modes (RBMs) associated with the outer tubes (whether semiconducting or metallic) *via* the mechanical wrapping and the strong charge transfer between DNA and the outer tubes support our interpretation that the bright luminescence and sharp absorption spectra come from only the inner tubes, and not from isolated SWNTs. The circumferentially wrapped DNA on the outer tubes of individually isolated DWNTs in an aqueous solution gives rise to strong charge transfer to the semiconducting and metallic outer tubes as well as to generating physical strain in the outer tubes.

KEYWORDS: double walled carbon nanotubes · single stranded DNA · Raman spectroscopy · luminescence

Double-walled carbon nanotubes (DWNTs) have attracted a great deal of attention[1] because their intrinsic coaxial structures make them mechanically, thermally, and structurally more stable than single walled carbon nanotubes (SWNTs).[2] Geometrically, the bufferlike function of the outer tubes in DWNTs allows the inner tubes to exhibit exciting transport and structural properties[3−6] that make them promising in the fabrication of field-effect transistors,[7−10] stable field emitters[11] and lithium ion batteries.[12] In addition, selective functionalization of the outer tubes makes DWNTs useful for anchoring semiconducting quantum dots[13] as well as for use as an effective multifunctional filler in producing tough, conductive transparent polymer films,[14] while the inner tubes with diameters below 0.9 nm preserve their excitonic transitions.[15] Up to now, the vibrational properties of the inner tubes in the solid form of a DWNT sample have been systematically studied using Raman spectroscopy as a characterization tool,[16−22] where strong Raman lines associated with the inner tubes have been used as a fingerprint for identifying the growth of the inner tubes in the hollow core of large diameter SWNT hosts.

On the other hand, optical studies on a density gradient-enriched DWNT solution[23] suggested that the luminescence originates not from the inner tube of the DWNT but from impurity SWNTs by referring to the absence of luminescence in peapod-grown DWNTs,[24] even though several studies reported bright and stable luminescence from the inner tubes in a sodium dodecylbenzene sulfonate (SDBS)-dispersed DWNT solution.[25−29] In this context, our group has confirmed the bright luminescence coming from the inner tube from peapod-grown DWNTs without the presence of any impurity SWNTs, in a DWNT sample that was prepared by thermally treating a peapod sample above 1700 °C in an argon atmosphere.[30] On this basis, it is expected that DWNTs will someday replace SWNTs in biomarkers[31] and optoelectronics[32] owing to their strong and stable luminescence.

Therefore, when considering the promising application potential of DWNTs as stable luminescent biomarkers, a long-time stable and homogeneously dispersed DWNT solution with a high biocompatibility should be prepared. In this sense, we have selected single-stranded DNA as the dispersing agent because DNA is well-known to be effective for dispersing and sorting

*Address correspondence to yak@endomoribu.shinshu-u.ac.jp.

Received for review December 21, 2009 and accepted January 25, 2010.

Published online January 29, 2010. 10.1021/nn901871g

© 2010 American Chemical Society

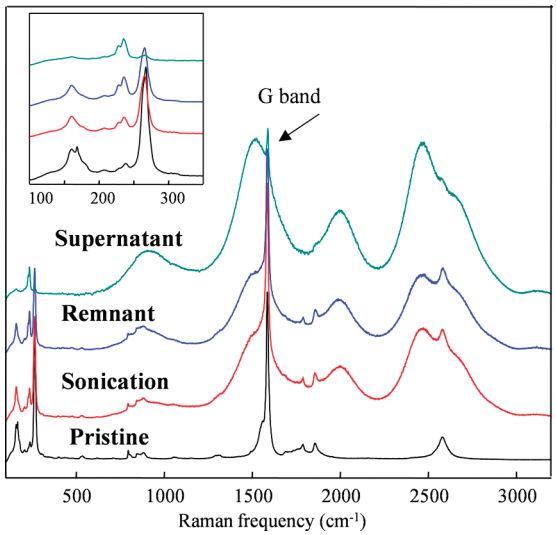

Figure 1. Raman/fluorescence spectra taken with laser excitation of 785 nm for pristine DWNTs, and for DNA-dispersed DWNT solutions at different dispersion states (sonicated, remnant, and supernatant). The inset shows the magnified low-frequency Raman spectra for the corresponding samples.

SWNTs[33−36] and the interaction of DNA with SWNTs has been studied both theoretically and experimentally.[37−44]

In this account, it is very important to understand the interaction between DNA and the outer tubes in a DWNT solution, where the inner tubes are structurally shielded by outer tubes, and where a possible charge transfer occurs from the outer tubes to the inner tubes, thereby affecting the luminescence from the inner tubes. We have thus prepared DNA-dispersed DWNT solutions at different dispersion states, and then carried out detailed Raman and luminescence spectroscopic studies on a DNA-dispersed DWNT aqueous solution in comparison to a corresponding SDBS-dispersed DWNT solution using three different laser lines (532, 633, and 785 nm). We observed intensified luminescence signals and as well as preserved radial breathing modes (RBMs) in the Raman spectra coming from the inner tubes in both individually dispersed DWNT solutions, though the RBMs coming from the outer tubes were severely depressed after DNA wrapping, regardless of the outer tube metallicity.

RESULTS AND DISCUSSION

We used highly pure (*ca.* 99%), highly crystalline DWNTs (absence of the D-band in their Raman spectra)[45] in which nanotubes with an outer diameter of *ca.* 1.6 nm were packed in hexagonal arrays within the bundles. Then we prepared a homogeneously dispersed DWNT aqueous solution using single stranded DNA, as described in our previous study.[46] Figure 1 shows Raman/fluorescence spectra taken with laser excitation of 785 nm for pristine DWNTs, and DNA-dispersed DWNT solutions at different dispersion states. From the Raman spectra of pristine DWNTs, we could see a strong G-band (E_{2g2} mode) at around 1592 cm^{-1}, while below 500 cm^{-1}, several RBMs (which correspond to a coherent vibration of the carbon atoms normal to the tube axis) could be seen along with the second order symmetry-allowed G′-band at around 2600 cm^{-1}.[47] However, by sonicating DWNTs in a DNA aqueous solution, several strong luminescence peaks start to appear, indicating that individually dispersed DWNTs are generated through the interaction with DNA, because we are not able to see bright luminescence from the bundled sample due to the presence of entrapped metallic (M) tubes which quench the luminescence.[48] Moreover, by concentrating individually isolated DWNTs in a DNA solution through the removal of thin bundled DWNTs using ultracentrifugation, we found that the intensity of the luminescence peaks becomes very strong and comparable to the intensity of the G-band in the supernatant sample.

Since the RBMs of SWNTs are well-known to provide information on the chirality and diameter,[49−51] the low-frequency Raman spectra is magnified (see inset in Figure 1). Because of their intrinsic coaxial geometries, DWNTs are able to have the four configurations (*i.e.*, S@S, S@M, M@S, and M@M, where S@M denotes a semiconducting (S) inner tube within a metallic (M) outer tube). Thus, by using a theoretical Kataura plot based on the extended tight binding exciton model for SWNTs,[52] we could assign the inner tubes with diameters of ca. 0.8 nm that are in resonance with 785 nm laser excitation to be S tubes, while the outer tubes with diameters of ca. 1.56 nm were identified to be M tubes. It is noteworthy that the RBM signals are arising from an ensemble of different DWNTs, and not from an individual DWNT. The intensity of the peak at 267 cm^{-1} decreases through a debundling process and finally disappears in individually isolated DWNTs. On the other hand, the frequencies and intensities of the RBM associated with the semiconducting inner tubes are constant regardless of the dispersion state of the DWNTs. However, the depressed intensity of the RBM at 160 cm^{-1} associated with the metallic outer tube is quite different from the behavior of the peak at 267 cm^{-1} because the outer tubes are in contact with DNA and their electronic structure is modified by charge transfer from the negatively charged DNA.

To understand the effect of DNA (which is known to helically wrap around carbon nanotubes)[34,35] on the RBMs and luminescence peaks in detail, we have compared Raman/luminescence spectra taken with the laser excitation of 785 nm for SDBS- and DNA-dispersed DWNT solutions (Figure 2). The strong luminescent peaks in the SDBS-dispersed DWNT solution could be assigned to the (6,4), (9,1), (8,3), (6,5) and (7,5) nanotubes.[53] Noticeably, the luminescence spectra of DNA-dispersed DWNT solution (Figure 2) are red-shifted compared to that of the SDBS-dispersed DWNT solu-

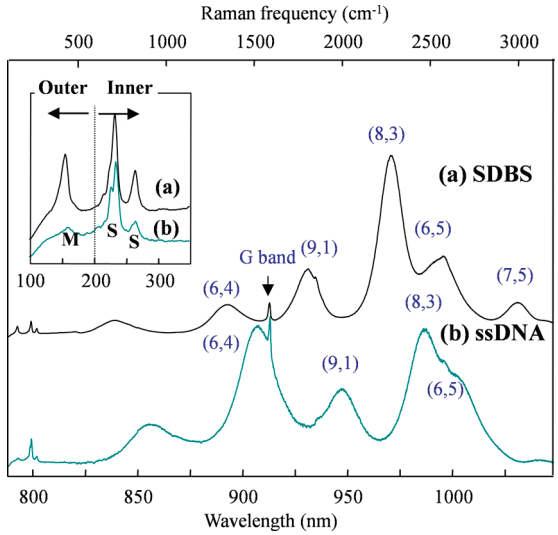

Figure 2. Comparative Raman/fluorescence spectra taken with laser excitation of 785 nm for SDBS- and DNA-dispersed DWNT supernatants. The inset shows the magnified low frequency Raman spectra, where M indicates metallic and S indicates semiconducting tubes.

tion. This shift should be explained by environmental dielectric screening effects,[54−58] since the accessibility of water to the surface of DWNTs in DNA-dispersed DWNTs is expected to be greater than for SDBS-dispersed DWNTs, thereby allowing water molecules to interact strongly with the outer tubes. In addition, a strong luminescence peak from the (8,3) tube is observed from the SDBS-dispersed DWNTs solution, while the (6,4) tube shows the strongest peak in the DNA-dispersed DWNT solution. This result suggests differences in DNA- and SDBS-dispersed DWNTs species due to their intrinsically different interactions with their wrapping molecules. This assumption is clearly verified in the drastic change of the RBMs for both solutions (see inset in Figure 2). The RBM intensity associated with the outer tube in the DNA-dispersed DWNT solution is highly depressed, whereas the corresponding RBM in the SDBS-dispersed DWNT solution maintains its intensity comparable to a pristine DWNT. This RBM depression can be explained by direct charge transfer from DNA to the outer tubes, thus filling states below the resonant van Hove singularity of the metallic outer tube of the DWNT, as previously demonstrated in the detailed Raman study carried out on individual semiconducting and metallic SWNTs.[59] Moreover, we observed an upshifted RBM frequency (*ca.* 4 cm^{-1}) associated with outer tubes, indicating that the circumferentially generated and concentrated stress due to the presence of the helically wrapped DNA along the outer surface of the DWNT suppresses the coherent RBM vibration of the carbon atoms in a direction normal to the tube axis. However, the absence of a change in the frequency of the RBMs associated with the inner tubes suggests the absence of stress transfer from the outer to the inner tubes, as evidenced by the fluorescence study of polyvinlypyrrolidone-dispersed DWNTs.[29] This result also supports the protective function of the outer tubes in DWNTs.

However, the depressed RBM intensity at 265 cm^{-1} in the DNA-dispersed solution is unexpected, because the protective effect of the outer tubes maintains the intensity of their RBMs which appear at around 240 cm^{-1}. Using the inverse relationship between the RBM frequency (ω) and the tube diameter (d) ($\omega = 218.3/d + 15.9$),[60] we are able to assign the two RBMs at 265 and 150 cm^{-1} as due to a semiconducting inner tube having a diameter of 0.88 nm and a metallic outer tube having a diameter of 1.63 nm (S@M DWNT), as confirmed by a resonance Raman study on isolated DWNTs.[61] Very recently, two separate Raman studies[62,63] showed a severely modified electronic structure for metallic SWNTs due to the presence of helically wrapped DNA, where water molecules activated a transition from metallic to a p-type semiconducting behavior in a SWNT. Therefore, in the case of the S@M DWNT configuration, strong charge transfer between the outer tube and the wrapped DNA is thought to be one of the reasons for the substantial depression of the RBM at 265 cm^{-1}.

Furthermore, to confirm the individually isolated state of the DWNTs in the supernatant, we have carried out photoluminescence mapping (PL), UV−vis absorption spectra, and TEM observations. The appearance of three strong PL peaks (corresponding to the inner tubes with chiralities (8,3), (7,5), and (10,2)) in the PL map (Figure 3a) indicates the presence of individually isolated DWNTs in the DNA solution. In addition, DWNTs dispersed in a DNA solution exhibited well-resolved and sharp optical absorption peaks due to their excitonic transitions between van Hove singularities (Figure 3b), thus indicating that individual nanotubes were isolated. The observed red-shifted E_{11} emis-

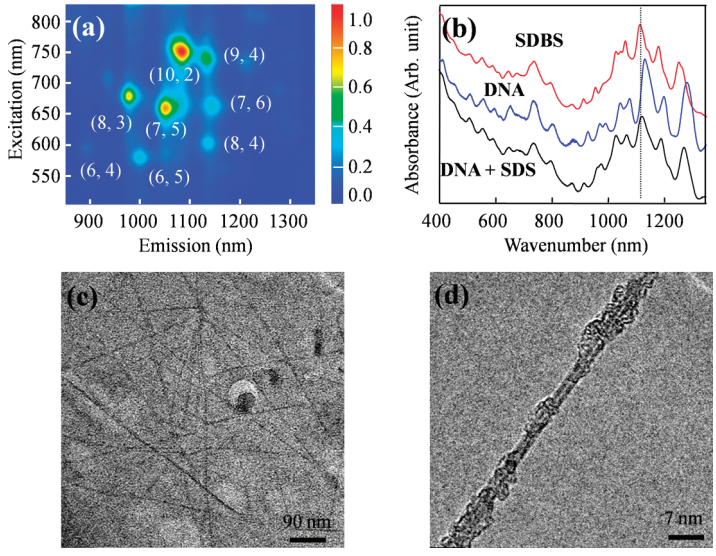

Figure 3. (a) PL map and (b) UV−visible absorption spectra of DNA-dispersed DWNT solution at pH = 8.0, (c, d) their corresponding TEM images. Note that DWNTs are individualized with the help of helically wrapped DNA. The color represents the PL intensity on a linear scale.

sion (*ca.* 45 meV) (Figure 3a) and UV absorption peaks (Figure 3b) as compared to the SDBS-dispersed DWNT solution are ascribed to their different environmental dielectric screening effects.[54−58] To confirm these effects, an SDS solution (1 wt %) was steadily added to the DNA-dispersed DWNT solution and then sonicated for 10 min. Interestingly, we then observed a blue shift in the DNA- and SDS-dispersed DWNT solution. Such a blueshift can be explained by the increased coverage of the DWNTs by surfactants resulting from the combination of long and helical DNA and particle-like SDS molecules on the outer surface of the outer tubes, which gives rise to a decreased dielectric constant. Visually, we have verified the individually dispersed DWNTs in low resolution TEM (Figure 3c). Interestingly, typical high resolution TEM (Figure 3d) revealed that DNA is helically wrapped along the outer surface of DWNT in an irregular pattern, and bare nanotube surfaces are partially present and allow water molecules to interact with the outer tube, which is closely related with the redshift of the E_{11} emission (Figure 3a) and absorption peaks (Figure 3b).

We also have measured Raman spectra using a laser excitation of 633 nm for pristine DWNTs, DNA-dispersed DWNT solutions at different dispersion states (Figure 4a). Here we could see a broad peak coming from the O−H stretching transitions of water molecules[64] at around 3300 cm^{-1} from the individually isolated DWNT solution. To see Raman changes in greater detail, we have magnified the RBMs below 400 cm^{-1}, the G-band and the G′-band (Figure 4b−d), respectively. According to the calculated diameter from the sharp RBMs (Figure 4b), we are able to assign two possible configurations (*i.e.*, dominantly S@S and partially M@S). We could see a severely depressed RBM intensity (which is associated with the semiconducting outer tube) at 150 cm^{-1} in the supernatant. Concurrently, the RBM associated with the metallic inner tube at 220 cm^{-1} is also depressed, while the RBM for (semiconducting inner tube) at 258 cm^{-1} retains its intensity and the RBM for semiconducting inner tube at 280 cm^{-1} is significantly intensified. These facts tell us that metallic inner tubes could be affected through charge transfer from DNA-wrapped outer tubes. When looking at the G band (Figure 4c), the broad and asymmetric Breit−Wigner−Fano (BWF) line[65] in the pristine DWNT sample is strongly depressed and shifted to a low frequency with the increasing dispersion state of the DWNTs in the DNA solution. In addition, the width of the G′ band is decreased for the individually isolated DWNTs in solution (Figure 4d).

Finally, we have measured Raman spectra using the 532 nm laser excitation for pristine DWNTs and DNA-dispersed DWNT solutions at different dispersion states (Figure 5a). With increasing the dispersion state of the DWNTs in DNA solution, the OH-stretching transitions from water molecules become intense consecutively. From the low-frequency Raman spectra (Figure 5b), we can easily assign the RBM at 265 cm^{-1} to a metallic inner tube and the RBM at 158 cm^{-1} to a semiconducting outer tube (in a M@S configuration). The

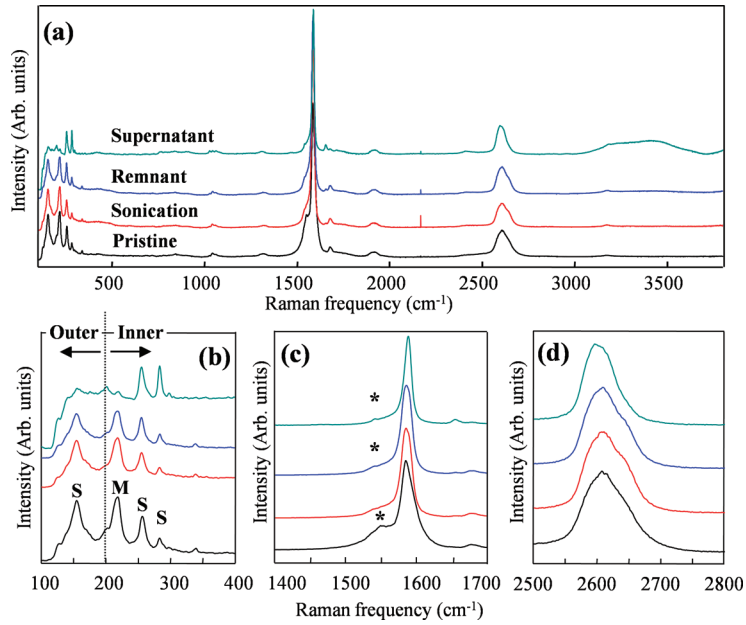

Figure 4. (a) Wide-range Raman spectra taken with laser excitation of 633 nm for pristine DWNTs, and for DNA-dispersed DWNT solutions at different dispersion states (sonicated, remnant, and supernatant), and their corresponding (b) radial breathing mode (where S indicates semiconducting and M indicates metallic tubes), (c) G-band (asterisk indicates the BWF line associated with metallic outer tubes) and (d) the G′-band Raman spectra, respectively.

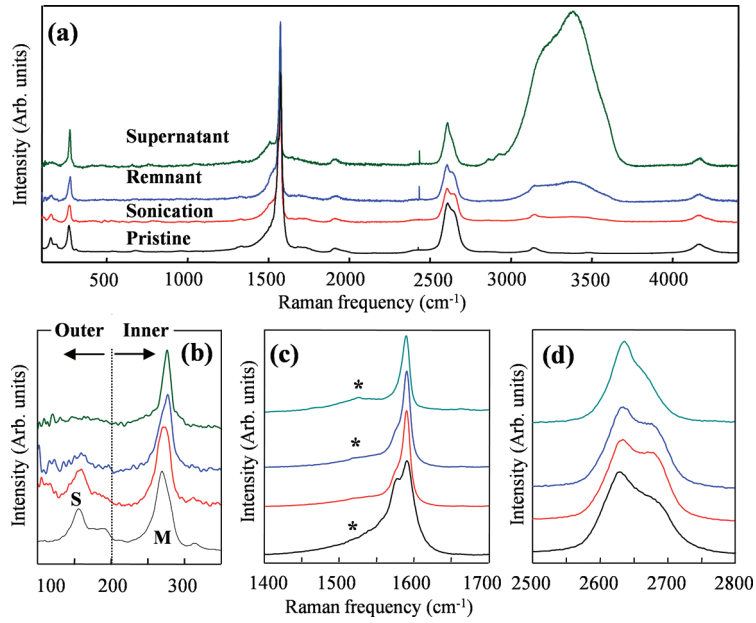

Figure 5. (a) Wide-range Raman spectra taken with laser excitation of 532 nm for pristine DWNT, and DNA-dispersed DWNT solutions at different dispersion states (sonicated, remnant, and supernatant), and their corresponding (b) radial breathing mode (where S indicates semiconducting and M indicates metallic tubes), (c) the G-band (asterisk indicates the BWF line associated with metallic inner tubes) and (d) the G′-band Raman spectra, respectively.

RBM intensity at 158 cm^{-1} decreases continuously with increasing dispersion state of the tubes, and finally disappears in the individually isolated DWNT solution. The G-band consists of two Lorentzian peaks at 1592 and 1572 cm^{-1} and a broad metallic tail at 1519 cm^{-1} because both the inner and outer tubes are resonant with the laser excitation of 532 nm. By increasing the dispersion state of the DWNTs in the DNA solution, we could see a consecutive decrease in the G-band coming from the semiconducting outer tubes at 1570 cm^{-1} (Figure 5c). Therefore, we could assign the strong G band at 1592 cm^{-1} to the metallic inner tubes with the clear observation of the broad and asymmetric BWF line at around 1525 cm^{-1} in the supernatant. As shown in Figure 5d, the G′-band of pristine DWNTs consists of two Lorentzian peaks. Two previous studies have assigned the Raman line at *ca.* 2630 cm^{-1} to the inner tubes and the Raman line at 2677 cm^{-1} to the outer tubes by analyzing the Raman spectra in peapod-derived DWNTs.[66,67] In addition, a recent study showed that the presence of defects in SWNTs was a reason for the evolution of the low frequency component of the G′ band.[68] For individual isolated DWNTs in the DNA solution, our results show that the outer tube-induced Raman line at 2677 cm^{-1} becomes highly depressed and correlated with the disappearance of the RBM.

CONCLUSIONS

Here we report, for the first time, detailed Raman/luminescence spectroscopic studies on ssDNA-dispersed DWNT solutions at different dispersion states, in comparison with an SDBS-dispersed DWNT solution using three different laser lines, in order to understand the interactions between DNA and the outer tubes, and the effect of these different DWNT environments on the vibrational and luminescence behaviors. By increasing the dispersion state of the DWNTs in an aqueous DNA solution, the luminescence peaks were intensified and shifted to longer wavelengths, indicating that DWNTs are individually dispersed in an aqueous solution, which is strongly supported by the strong PL map and the sharp absorption spectra as well as high-resolution TEM observations. Noticeably, we observed cases of completely depressed RBM intensities associated with the outer tubes (regardless of their metallicity) for three configurations of DWNTs (S@M, S@S, and M@S). This result strongly supports the interpretation that the evolved luminescence and sharp absorption peaks (Figure 3a,b) solely come from the semiconducting inner tubes of the DWNTs, not from impurity SWNTs. In addition, the metallic inner tubes are partially affected by the DNA-wrapped outer tubes. Conclusively, the circumferentially wrapped DNA on the outer tubes of individually isolated DWNTs in an aqueous solution gives rise to strong charge transfer to the semiconducting and metallic outer tubes as well as generating physical strain in the outer tubes. Therefore, we envisage that DNA-dispersed DWNTs are highly promising for producing strong and stable luminescence signals as well as for high yield optoelectronics applications.

EXPERIMENTAL SECTION

We purchased herring sperm DNA (degraded free acid) from Nacalai Tesque, Inc. To prepare single stranded DNA (ssDNA), we carried out the following procedures: first, we obtained short DNA sequences with 200 base pairs, we dissolved 10 mg of herring sperm DNA in 10 mL of distilled water under mild sonication for 5 min, and then added 1 mL of 1 N sodium hydroxide solution. Following incubation of the solution for 5 min, we neutralized the DNA solution by adding 1 mL of 1 N hydrochloric acid and subsequently stabilized the DNA solution by adding 2 mL of 1 M trihydrochloric buffer solution (pH = 8). The prepared highly pure DWNTs (*ca.* 3 mg) were individually dispersed (or isolated) in an aqueous solution (10 mL) with the help of ssDNA wrapping under strong sonication (KUBOTA UP50H, *ca.* 470 W/cm^2) for 1 h at 4 °C, and subsequent ultracentrifugation (Optima Max-XP, Beckman Coulter, 240000*g*). Their supernatant (70%), rich with isolated nanotubes, was characterized in solution by transferring these solutions to a quartz cuvette. Raman spectra at 785 nm excitations were obtained using a Renishaw setup fitted with a macroscopic sampling kit. We also obtained Raman spectra using 532 and 633 nm laser excitations produced by a Kaiser HoloLab5000 system. To confirm the individually dispersed DWNTs in the DNA solution, we measured their UV−vis absorption spectra (SolidSpec-3700, Shimazu) and photoluminescence maps (NIR-PL system, Shimazu). Finally, we used TEM (JEOL2010FEF) for studying the dispersed state of the DWNTs.

Acknowledgment. We acknowledge the support from the CLUSTER (second stage) and the MEXT grants (Nos. 19002007, and 20510096). M.S.D. acknowledges support from NSF/DMR 07-04197. J.H.K. acknowledges the support of Shinshu University Global COE Program "International Center of Excellence on Fiber Engineering". R.S. acknowledges MEXT Grant No. 20241023. J.S.P. acknowledges Global COE Program of Tohoku University.

REFERENCES AND NOTES

1. Pfeiffer, R.; Pichler, T.; Kim, Y. A.; Kuzmany, H. Double-Wall Carbon Nanotubes . *Carbon Nanotubes: Advanced Topics in the Synthesis, Structure, Properties and Applications*; Jorio, A., Dresselhaus, M. S., Dresselhaus, G., Eds.; Springer: New York, 2008; pp 495−530.
2. Kim, Y. A.; Muramatsu, H.; Hayashi, T.; Endo, M.; Terrones, M.; Dresselhaus, M. S. Thermal Stability and Structural Changes of Double-Walled Carbon Nanotubes by Heat Treatment. *Chem. Phys. Lett.* **2004**, *398*, 87–92.
3. Pfeiffer, R.; Kuzmany, H.; Kramberger, C.; Schaman, C.; Pichler, T.; Kataura, H.; Achiba, Y.; Kürti, J.; Zólyomi, V. Unusual High Degree of Unperturbed Environment in the Interior of Single-Wall Carbon Nanotubes. *Phys. Rev. Lett.* **2003**, *90*, 225501.
4. Herández, E.; Meunier, V.; Smith, B. W.; Rurali, R.; Terrones, H.; Buongiorno Nardelli, M.; Terrones, M.; Luzzi, D. E.; Charlier, J.-C. Fullerene Coalescence in Nanopeapods: A Path to Novel Tubular Carbon. *Nano Lett.* **2003**, *3*, 1037–1042.

5. Kavan, L.; Dunsch, L.; Kataura, H. Electrochemical Tuning of Electronic Structure of Carbon Nanotubes and Fullerene Peapods. *Carbon* **2004**, *42*, 1011–1019.
6. Souza Filho, A. G.; Meunier, V.; Terrones, M.; Sumpter, B. G.; Barros, E. B.; Villalpando-Paez, F.; Mendes Filho, J.; Kim, Y. A.; Muramatsu, H.; Hayashi, T.; *et al*. Selective Tuning of the Electronic Properties of Coaxial Nanocables through Exohedral Doping. *Nano Lett.* **2007**, *7*, 2383–2388.
7. Shimada, T.; Sugai, T.; Ohno, Y.; Kishimoto, S.; Mizutani, T.; Yoshida, H.; Okazaki, T.; Shinohara, H. Double-Wall Carbon Nanotube Field-Effect Transistors: Ambipolar Transport Characteristics. *Appl. Phys. Lett.* **2004**, *84*, 2412.
8. Yuan, S.; Zhang, Q.; Shimamoto, D.; Muramatsu, H.; Hayashi, T.; Kim, Y. A.; Endo, M. Hysteretic Transfer Characteristics of Double-Walled and Single-Walled Carbon Nanotube Field-Effect Transistors. *Appl. Phys. Lett.* **2007**, *9*, 1–143118.
9. Liu, K. H.; Wang, W. L.; Xu, Z.; Bai, X. D.; Wang, E. G.; Yao, Y. G.; Zhang, J.; Liu, Z. F. Chirality-Dependent Transport Properties of Double-Walled Nanotubes Measured *in Situ* on Their Field-Effect Transistors. *J. Am. Chem. Soc.* **2009**, *131*, 62–63.
10. Yuan, S.; Zhang, Q.; You, Y.; Shen, Z.-X.; Shimamoto, D.; Endo, M. Correlation between *in Situ* Raman Scattering and Electrical Conductance for an Individual Double-Walled Carbon Nanotube. *Nano Lett.* **2009**, *9*, 383–387.
11. Ha, B.; Shin, D. H.; Park, J.; Lee, C. J. Electronic Structure and Field Emission Properties of Double-Walled Carbon Nanotubes Synthesized by Hydrogen Arc Discharge. *J. Phys. Chem. C* **2009**, *112*, 430–435.
12. Kim, Y. A.; Kojima, M.; Muramatsu, H.; Umemoto, S.; Watanabe, T.; Yoshida, K.; Sato, K.; Ikeda, T.; Hayashi, T.; Endo, M.; *et al*. *In Situ* Raman Study on Single- and Double-Walled Carbon Nanotubes as a Function of Lithium Insertion. *Small* **2006**, *2*, 667–676.
13. Kim, Y. A.; Muramatsu, H.; Park, K. C.; Shimamoto, D.; Jung, Y. C.; Kim, J. H.; Hayashi, T.; Saito, Y.; Endo, M.; Terrones, M.; *et al*. CdSe Quantum Dot-Decorated Double Walled Carbon Nanotubes: The Effect of Chemical Moieties. *Appl. Phys. Lett.* **2008**, *93*, 051901.
14. Jung, Y. C.; Shimamoto, D.; Muramatsu, H.; Kim, Y. A.; Hayashi, T.; Terrones, M.; Endo, M. Robust, Conducting, and Transparent Polymer Composites Using Surface-Modified and Individualized Double-Walled Carbon Nanotubes. *Adv. Mater.* **2008**, *20*, 4509–4512.
15. Hayashi, T.; Shimamoto, D.; Kim, Y. A.; Muramatsu, H.; Okino, F.; Touhara, H.; Shimada, T.; Miyauchi, Y.; Maruyama, S.; Terrones, M.; *et al*. Selective Optical Property Modification of Double-Walled Carbon Nanotubes by Fluorination. *ACS Nano* **2008**, *2*, 485–488.
16. Bandow, S.; Takizawa, M.; Hirahara, K.; Yudasaka, M.; Iijima, S. Raman Scattering Study of Double-Wall Carbon Nanotubes Derived from the Chains of Fullerenes in Single-Wall Carbon Nanotubes. *Chem. Phys. Lett.* **2001**, *337*, 48–54.
17. Pfeiffer, R.; Simon, F.; Kuzmany, H.; Popov, V. N. Fine structure of the Radial Breathing Mode of Double-Wall Carbon Nanotubes. *Phys. Rev. B* **2005**, *72*, 161404.
18. Bandow, S.; Hiraoka, T.; Yumura, T.; Hirahara, K.; Shinohara, H.; Iijima, S. Raman Scattering Study on Fullerene Derived Intermediates Formed within Single-Wall Carbon Nanotube: From Peapod to Double-Wall Carbon Nanotube. *Chem. Phys. Lett.* **2004**, *384*, 320–325.
19. Kramberger, C.; Waske, A.; Biedermann, K.; Pichler, T.; Gemming, T.; Buchner, B.; Kataura, H. Tailoring Carbon Nanostructures *via* Temperature and Laser Irradiation. *Chem. Phys. Lett.* **2005**, *407*, 254–259.
20. Pfeiffer, R.; Holzweber, M.; Peterlik, H.; Kuzmany, H.; Liu, Z.; Suenaga, K.; Kataura, H. Dynamics of Carbon Nanotube Growth from Fullerenes. *Nano Lett.* **2007**, *7*, 2428–2434.
21. Zolyomi, V.; Simon, F.; Rusznyak, A.; Pfeiffer, R.; Peterlik, H.; Kuzmany, H.; Kurt, J. Inhomogeneity of ^{13}C Isotope Distribution in Isotope Engineered Carbon Nanotubes: Experiment and Theory. *Phys. Rev. B* **2007**, *75*, 195419.
22. Kuzmany, H.; Plank, W.; Pfeiffer, R.; Simon, F. Raman Scattering from Double-Walled Carbon Nanotubes. *J. Raman Spectrosc.* **2008**, *39*, 134–140.
23. Green, A. A.; Hersam, M. C. Processing and Properties of Highly Enriched Double-Wall Carbon Nanotubes. *Nat. Nanotechnol.* **2009**, *4*, 64–70.
24. Okazaki, T.; Bandow, S.; Tamura, G.; Fujita, Y.; Iakoubovskii, K.; Kazaoui, S.; Minami, N.; Saito, T.; Suenaga, K.; Iijima, S. Photoluminescence Quenching in Peapod-Derived Double-Walled Carbon Nanotubes. *Phys. Rev. B* **2006**, *74*, 153404.
25. Kishi, N.; Kikuchi, S.; Ramesh, P.; Sugai, T.; Watanabe, Y.; Shinohara, H. Enhanced Photoluminescence from Very Thin Double-Wall Carbon Nanotubes Synthesized by the Zeolite-CCVD Method. *J. Phys. Chem. B* **2006**, *110*, 24816–24821.
26. Hertel, T.; Hagen, A.; Talalaev, V.; Arnold, K.; Hennrich, F.; Kappes, M.; Rosenthal, S.; McBride, J.; Ulbricht, H.; Flahaut, E. Spectroscopy of Single- and Double-Wall Carbon Nanotubes in Different Environments. *Nano Lett.* **2005**, *5*, 511–514.
27. Iakoubovskii, K.; Minami, N.; Kazaoui, S.; Ueno, T.; Miyata, Y.; Yanagi, K.; Kataura, H.; Ohshima, S.; Saito, T. IR-Extended Photoluminescence Mapping of Single-Wall and Double-Wall Carbon Nanotubes. *J. Phys. Chem. B* **2006**, *110*, 17420–17424.
28. Iakoubovskii, K.; Minami, N.; Ueno, T.; Kazaoui, S.; Kataura, H. Optical Characterization of Double-Wall Carbon Nanotubes: Evidence for Inner Tube Shielding. *J. Phys. Chem. C* **2008**, *112*, 11194–11198.
29. Shimamoto, D.; Muramatsu, H.; Hayashi, T.; Kim, Y. A.; Endo, M.; Park, J. S.; Saito, R.; Terrones, M.; Dresselhaus, M. S. Strong and Stable Photoluminescence from the Semiconducting Inner Tubes within Double Walled Carbon Nanotubes. *Appl. Phys. Lett.* **2009**, *94*, 083016.
30. Muramatsu, H.; Hayashi, T.; Kim, Y. A.; Shimamoto, D.; Endo, M.; Meunier, V.; Sumpter, B. G.; Terrones, M.; Dresselhaus, M. S. Bright Photoluminescence from the Inner Tubes of "Peapod"-Derived Double-Walled Carbon Nanotubes. *Small* **2009**, *5*, 2678–2682.
31. Heller, D. A.; Baik, S.; Eurell, T. E.; Strano, M. S. Single-Walled Carbon Nanotube Spectroscopy in Live Cells: Towards Long-Term Labels and Optical Sensors. *Adv. Mater.* **2005**, *17*, 2793–2799.
32. E. Itkis, M.; Boronndics, F.; Yu, A.; Haddon, R. C. Bolometric Infrared Photoresponse of Suspended Single-Walled Carbon Nanotube Films. *Science* **2006**, *312*, 413–416.
33. Nakashima, N.; Okuzono, S.; Murakami, H.; Nakai, T.; Yoshikawa, K. DNA Dissolves Single-Walled Carbon Nanotubes in Water. *Chem. Lett.* **2003**, *32*, 456–457.
34. Zheng, M.; Jagota, A.; Semke, E. D; Diner, B. A.; McLean, R. S.; Lustig, S. R.; Richardson, R. E.; Tassi, N. G. DNA-Assisted Dispersion and Separation of Carbon Nanotubes. *Nat. Mater.* **2003**, *2*, 338–342.
35. Zheng, M.; Jagota, A.; Strano, M. S.; Santos, A. P.; Barone, P.; Chou, S. G.; Diner, B. A.; Dresselhaus, M. S.; Mclean, R. S.; Onoa, G. B.; *et al*. Structure-Based Carbon Nanotube Sorting by Sequence-Dependent DNA Assembly. *Science* **2003**, *302*, 1545–1548.
36. Tu, X.; Manohar, S.; Jagota, A.; Zheng, M. DNA Sequence Motifs for Structure-Specific Recognition and Separation of Carbon Nanotubes. *Nature* **2009**, *460*, 250–253.
37. Strano, M. S.; Zheng, M.; Jagota, A.; Onoa, G. B.; Heller, D. A.; Barone, P. W.; Usrey, M. L. Understanding the Nature of the DNA-Assisted Separation of Single-Walled Carbon Nanotubes Using Fluorescence and Raman Spectroscopy. *Nano Lett.* **2004**, *4*, 543–550.
38. Zheng, M.; Diner, B. A. Solution Redox Chemistry of Carbon Nanotubes. *J. Am. Chem. Soc.* **2004**, *126*, 15490–15494.
39. Fantini, C.; Jorio, A.; Santos, A. P.; Peressinotto, V. S. T.; Pimenta, M. A. Characterization of DNA-Wrapped Carbon Nanotubes by Resonance Raman and Optical Absorption Spectroscopies. *Chem. Phys. Lett.* **2007**, *439*, 138–142.

40. Zhao, X.; Johnson, J. K. Simulation of Adsorption of DNA on Carbon Nanotubes. *J. Am. Chem. Soc.* **2007**, *129*, 10438–10445.
41. Meng, S.; Maragakis, P.; Papaloukas, C.; Kaxiras, E. DNA Nucleoside Interaction and Identification with Carbon Nanotubes. *Nano Lett.* **2007**, *7*, 45–50.
42. Chen, Y.; Liu, H.; Ye, T.; Kim, J.; Mao, C. DNA-Directed Assembly of Single-Wall Carbon Nanotubes. *J. Am. Chem. Soc.* **2007**, *129*, 8696–8697.
43. Fantini, C.; Jorio, A.; Santos, A. P.; Peressinotto, V. S. T.; Pimenta, M. A. Characterization of DNA-Wrapped Carbon Nanotubes by Resonance Raman and Optical Absorption Spectroscopies. *Chem. Phys. Lett.* **2007**, *439*, 138–142.
44. Fantini, C.; Cassimiro, J.; Peressinotto, V. S. T.; Plentz, F.; Souza Filho, A. G.; Furtado, C. A.; Santos, A. P. Investigation of the Light Emission Efficiency of Single-Wall Carbon Nanotubes Wrapped with Different Surfactants. *Chem. Phys. Lett.* **2009**, *473*, 96–101.
45. Endo, M.; Muramatsu, H.; Hayashi, T.; Kim, Y. A.; Terrones, M.; Dresselhaus, M. S. 'Buckypaper' from Coaxial Nanotubes. *Nature* **2005**, *433*, 476.
46. Kim, J. H.; Kataoka, M.; Kim, Y. A.; Shimamoto, D.; Muramatsu, H.; Hayashi, T.; Endo, M.; Terrones, M.; Dresselhaus, M. S. Diameter-Selective Separation of Double-Walled Carbon Nanotubes. *Appl. Phys. Lett.* **2008**, *93*, 223107.
47. Rao, A. M.; Richter, E.; Bandow, S.; Chase, B.; Eklund, P. C.; Williams, K. W.; Menon, M.; Subbaswamy, K. R.; Thess, A.; Smalley, R. E.; *et al*. Diameter-Selective Raman Scattering from Vibrational Modes in Carbon Nanotubes. *Science* **1997**, *275*, 187–191.
48. O'Connell, M. J.; Bachilo, S. M.; Huffman, C. B.; Moore, V. C.; Strano, M. S.; Haroz, E. H.; Rialon, K. L.; Boul, P. J.; Noon, W. H.; Kittrell, C.; *et al*. Band Gap Fluorescence from Individual Single-Walled Carbon Nanotubes. *Science* **2002**, *297*, 593–596.
49. Heller, D. A.; Barone, P. W.; Swanson, J. P.; Mayrhofer, R. M.; Strano, M. S. Using Raman Spectroscopy to Elucidate the Aggregation State of Single-Walled Carbon Nanotubes. *J. Phys. Chem. B* **2004**, *108*, 6905–6909.
50. Araujo, P. T.; Fantini, C.; Lucchese, M. M.; Dresselhaus, M. S.; Jorio, A. The Effect of Environment on the Radial Breathing Mode of Supergrowth Single Wall Carbon Nanotubes. *Appl. Phys. Lett.* **2009**, *95*, 261902.
51. Jorio, A.; Santos, A. P.; Ribeiro, H. B.; Fantini, C.; Souza, M.; Vieira, J. P. M.; Furtado, C. A.; Jiang, J.; Saito, R.; Balzano, L.; *et al*. Quantifying Carbon-Nanotube Species with Resonance Raman Scattering. *Phys. Rev. B* **2005**, *72*, 075207.
52. Jiang, J.; Saito, R.; Samsonidze, G. G.; Jorio, A; Chou, S. G.; Dresselhaus, G.; Dresselhaus, M. S. Chirality Dependence of Exciton Effects in Single-Wall Carbon Nanotubes: Tight-Binding Model. *Phys. Rev. B* **2007**, *75*, 035407.
53. Bachilo, S. M.; Strano, M. S.; Kittrell, C.; Hauge, R. H.; Smalley, R. E.; Weisman, R. B. Structure-Assigned Optical Spectra of Single-Walled Carbon Nanotubes. *Science* **2002**, *298*, 2361–2366.
54. Lefebvre, J.; Fraser, J. M.; Homma, Y.; Finnie, P. Photoluminescence from Single-Walled Carbon Nanotubes: A Comparison between Suspended and Micelle-Encapsulated Nanotubes. *Appl. Phys. A: Mater. Sci. Process.* **2004**, *78*, 1107–1110.
55. Finnie, P.; Homma, Y.; Lefebvre, J. Band-Gap Shift Transition in the Photoluminescence of Single-Walled Carbon Nanotubes. *Phys. Rev. Lett.* **2005**, *94*, 247401.
56. Ohno, Y.; Iwasaki, S.; Murakami, Y.; Kishimoto, S.; Maruyama, S.; Mizutani, T. Chirality-Dependent Environmental Effects in Photoluminescence of Single-Walled Carbon Nanotubes. *Phys. Rev. B* **2006**, *73*, 235427.
57. Arnold, K.; Lebedkin, S.; Kowski, O.; Hennrich, F.; Kappes, M. M. Matrix-Imposed Stress-Induced Shifts in the Photoluminescence of Single-Walled Carbon Nanotubes at Low Temperatures. *Nano Lett.* **2004**, *4*, 2349–2354.
58. Miyauchi, Y.; Saito, R.; Sato, K.; Ohno, Y.; Iwasaki, S.; Mizutani, T.; Jiang, J.; Maruyama, S. Dependence of Exciton Transition Energy of Single-Walled Carbon Nanotubes on Surrounding Dielectric Materials. *Chem. Phys. Lett.* **2007**, *442*, 394–399.
59. Kalbac, M.; Farhat, H.; Kavan, L.; Kong, J.; Sasaki, K.; Saito, R.; Dresselhaus, M. S. Electrochemical Charging of Individual Single-Walled Carbon Nanotubes. *ACS Nano* **2009**, *3*, 2320–2328.
60. Endo, M.; Kim, Y. A.; Hayashi, T.; Muramatsu, H.; Terrones, M.; Saito, R.; Villalpando-Paez, F.; Chou, S. G.; Dresselhaus, M. S. Nanotube Coalescence-Inducing Mode: A Novel Vibrational Mode in Carbon Systems. *Small* **2006**, *2*, 1031–1036.
61. Villalpando-Paez, F.; Son, H.; Nezich, D.; Hsieh, Y. P.; Kong, J.; Kim, Y. A.; Shimamoto, D.; Muramatsu, H.; Hayashi, T.; Endo, M.; *et al*. Raman Spectroscopy Study of Isolated Double-Walled Carbon Nanotubes with Different Metallic and Semiconducting Configurations. *Nano Lett.* **2008**, *8*, 3879–3886.
62. Shoda, M.; Bandow, S.; Maruyama, Y.; Iijima, S. Probing Interaction between ssDNA and Carbon Nanotubes by Raman Scattering and Electron Microscopy. *J. Phys. Chem. C* **2009**, *113*, 6033–6036.
63. Cha, M.; Jung, S.; Cha, M.-H.; Kim, G.; Ihm, J.; Lee, J. Reversible Metal-Semiconductor Transition of ssDNA-Decorated Single-Walled Carbon Nanotubes. *Nano Lett.* **2009**, *9*, 1345–1349.
64. Eisenberg, D.; Kauzmann, W. *The Structure and Properties of Water*; Oxford University Press: Oxford, U.K., 2005.
65. Rao, A. M.; Eklund, P. C.; Bandow, S.; Thess, A.; Smalley, R. E. Evidence for Charge Transfer in Doped Carbon Nanotube Bundles from Raman Scattering. *Nature* **1997**, *388*, 257–259.
66. Kalbac, M.; Kavan, L.; Zukalova, M.; Dunsch, L. Electrochemical Tuning of High Energy Phonon Branches of Double Wall Carbon Nanotubes. *Carbon* **2004**, *42*, 2915–2920.
67. Pfeiffer, P.; Kuzmany, H.; Simon, F.; Bokova, S. N.; Obraztsova, E. Resonance Raman Scattering from Phonon Overtones in Double-Wall Carbon Nanotubes. *Phys. Rev. B* **2005**, *71*, 155409.
68. Maciel, I. O.; Anderson, N.; Pimenta, M. A.; Hartschuh, A.; Qian, H. H.; Terrones, M.; Terrones, H.; Campos-Delgado, J.; Rao, A. M.; Novotny, L.; *et al*. Electron and phonon renormalization near charged defects in carbon nanotubes. *Nat. Mater.* **2008**, *7*, 878–883.